



# Porphyrin Containing Polymersomes with Enhanced ROS Generation Efficiency: In Vitro Evaluation

Myrto Kyropoulou, Stefano Di Leone, Angelo Lanzilotto, Edwin C. Constable, Catherine E. Housecroft, Wolfgang P. Meier,\* and Cornelia G. Palivan\*

Porphyrins are molecules possessing unique photophysical properties making them suitable for application in photodynamic therapy. The incorporation of porphyrins into natural or synthetic nano-assemblies such as polymersomes is a strategy to improve and prolong their therapeutic capacities and to overcome their limitations as therapeutic and diagnostic agents. Here, 5,10,15,20-tetrakis(1-(6-ethoxy-6-oxohexyl)-4-pyridin-1-yl)-21H,23H-porphyrin tetrabromide porphyrin is inserted into polymersomes in order to demonstrate that the encapsulation enhances its ability to generate highly reactive singlet oxygen ( $^1\text{O}_2$ ) upon irradiation in vitro. The photoactivation of the free and polymersome-encapsulated porphyrin is evaluated by electron spin resonance and cell viability assays on three different mammalian cell lines. The results indicate that by encapsulating the porphyrin, a controlled ROS delivery within the cells is achieved, at the same time avoiding side effects such as dark toxicity, non-specific porphyrin release and over time decreased activity in vitro. This work focuses on showing a not-toxic model system for modern therapeutic nanomedicine, which works under mild irradiation and dosage conditions.

with subsequent damage to the cell components and consequent cell death.<sup>[1]</sup> PDT can be used to target tumor cells and is typically utilized in a combination therapy regime, together with other modalities such as radiotherapy, chemotherapy, and surgery. To optimize cell damage in the tumor and prevent significant collateral damage to healthy cells, the PS should be specifically localized in the pathogenic region. The lifetime and mean diffusion lengths of different ROS are very variable and localization will ensure that illumination generates ROS close to, at the surface of, or inside malignant tumor cells.


Of particular interest for development of efficient PDT systems are porphyrins because the photochemical and photophysical properties may be tuned through modification of the central metal ion (if present) or through peripheral substituents.<sup>[2–5]</sup> However, despite the great

## 1. Introduction

Photodynamic therapy (PDT) is an important non-invasive therapeutic technique which requires three components: a light source, a photosensitizer (PS), and dioxygen ( $\text{O}_2$ ). The mechanism involves the excitation of the PS, by illumination with an appropriate light source. The excited state of the PS can react with triplet dioxygen ( $^3\text{O}_2$ ), for example, inside mammalian cells, and convert it into reactive oxygen species (ROS). These reactive oxygen species, such as singlet dioxygen ( $^1\text{O}_2$ ), are cytotoxic and result in the oxidative stress of the target cells,

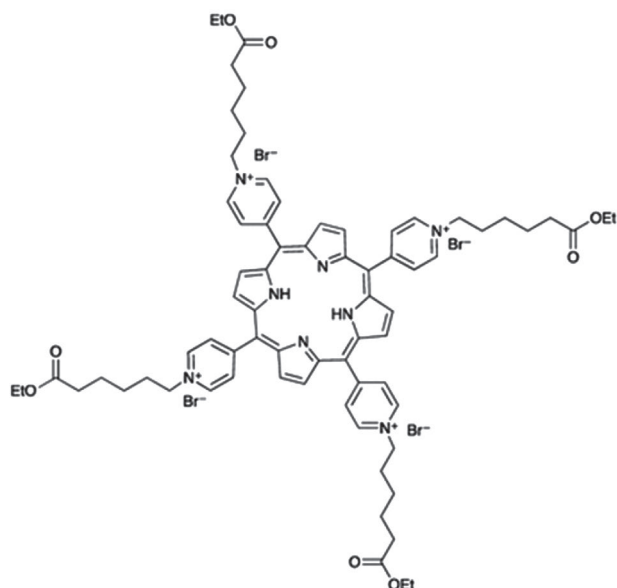
potential of porphyrins as photosensitizers, these compounds possess crucial limitations in terms of biomedical application<sup>[6,7]</sup> such as a high dark toxicity, rather low activity under physiological conditions and typically poor water solubility. Efficient strategies to overcome these limitations and at the same time harness the beneficial properties of porphyrins are the (bio)-conjugation of the porphyrin to natural or synthetic polymers<sup>[8–11]</sup> or their incorporation in biocompatible nanocarriers. Nanocarriers suitable for PDT materials include organic and inorganic nanoparticles,<sup>[12–17]</sup> liposomes,<sup>[18–21]</sup> and block copolymer-based vesicles or micelles.<sup>[22–24]</sup> Synthetic vesicles with sizes in the nanometer range, so-called polymersomes, are particularly appealing as carriers because they can be prepared with desired properties,<sup>[25]</sup> such as biocompatibility, possess an inner cavity where water-soluble photosensitizers can be encapsulated,<sup>[26]</sup> membranes allowing the entrapment of a hydrophobic photosensitizer and exhibit improved mechanical stability and robustness compared to liposomes.<sup>[27]</sup> There are a few examples of porphyrin-incorporating polymersomes, mostly concerning the non-covalent loading of the hydrophobic membrane with water insoluble porphyrins.<sup>[11,28–33]</sup> The aim of those studies was to use the photophysical properties of the porphyrins to improve in vivo imaging. We have previously reported the synthesis and characterization of a water soluble tetra-N-alkylpyridinoporphyrrin tetrabromide (TPyCP) (Scheme 1) which efficiently generates singlet oxygen both free

M. Kyropoulou, S. Di Leone, Dr. A. Lanzilotto<sup>[†]</sup>, Prof. E. C. Constable, Prof. C. E. Housecroft, Prof. W. P. Meier, Prof. C. G. Palivan  
Department of Chemistry  
University of Basel  
Mattenstrasse 24a 4058 Basel, Switzerland  
E-mail: [wolfgang.meier@unibas.ch](mailto:wolfgang.meier@unibas.ch); [cornelia.palivan@unibas.ch](mailto:cornelia.palivan@unibas.ch)

 The ORCID identification number(s) for the author(s) of this article can be found under <https://doi.org/10.1002/mabi.201900291>.

<sup>[†]</sup>Present address: Faculty of Pharmaceutical Sciences, University of British Columbia, 2405 Wesbrook Mall BC V6T 1Z3, Vancouver, Canada  
© 2019 The Authors. Published by WILEY-VCH Verlag GmbH & Co. KGaA, Weinheim. This is an open access article under the terms of the Creative Commons Attribution License, which permits use, distribution and reproduction in any medium, provided the original work is properly cited.

DOI: 10.1002/mabi.201900291



**Scheme 1.** Structure of the photosensitizer TPyCP.

in solution and when encapsulated in polymersomes.<sup>[34]</sup> TPyCP possesses charged functional groups which make it water-soluble, a necessary property for its incorporation into the inner aqueous cavity of the polymersomes.

Upon irradiation, TPyCP was able to eliminate the *E. Coli* bacteria both in solution and when encapsulated into PMOXA-PDMS-PMOXA polymersomes. For PDT application it is necessary to further investigate the behavior of this PS in mammalian cell lines, which are more complex and sensitive than bacteria. In this study, we present the photoactivation of dioxygen by TPyCP, both free in solution and encapsulated in polymersomes, and evaluate the efficiency of generation of reactive oxygen species in three different epithelial cell lines (HeLa, HEK 293T, and HepG2). We have chosen three cancer cell lines with different morphologies, sensitivities, originating from different tissues because we wanted to evaluate if they respond different to ROS and to get an idea of which cells line or lines responds better to our system. Porphyrin encapsulated inside the inner aqueous cavity of polymersomes generates singlet oxygen upon irradiation, and as the synthetic

membrane is permeable to ROS,<sup>[35,36]</sup> allowing their external diffusion. In addition, polymersomes formed from PMOXA-PDMS-PMOXA amphiphilic block copolymer are known to have a membrane which is thick, robust and stable enough to prevent any porphyrin leakage.<sup>[26,37,38]</sup> As a result, the toxic porphyrin<sup>[6,8]</sup> remains inside the polymersomes without any cytotoxic effect in the absence of irradiation. Only upon irradiation, are ROS generated in situ inside the cavity of polymersomes and reach the tested cells that we upon diffusion through the synthetic membrane. This is a requisite for a controlled effect in medical applications such as PDT. Moreover, the encapsulation enhances the ability of the porphyrin to constantly produce ROS, whereas when it is free in solution this degrades over time. The advantage of selecting TPyCP as photosensitizer is its ability to generate singlet oxygen under irradiation with a red (660 nm) LED, which is more affordable than a red laser and milder than the UV-irradiation conditions for typical PDT treatment.<sup>[39]</sup> To monitor the ROS generation in solution and in vitro we used spin traps and electron spin resonance spectroscopy (ESR).<sup>[40]</sup> Our interest was to make this porphyrin suitable for cellular uptake with negligible cytotoxicity and facilitate a controlled and continuous ROS generation in accordance with the demands of modern nanomedicine towards the advancement of PDT treatment.

## 2. Results and Discussion

### 2.1. Formation and Stability of TPyCP Containing Polymersomes

TPyCP containing polymersomes were formed by self-assembly of the triblock copolymer PMOXA<sub>6</sub>-PDMS<sub>34</sub>-PMOXA<sub>6</sub> in the presence of TPyCP using the film rehydration method.<sup>[38,41]</sup> According to DLS measurements and TEM micrographs (Figure S1, Supporting Information) the obtained polymersomes had the shape of hollow spheres with hydrodynamic radii ( $R_h$ ) around 100 nm (Figures S3 and S4, Supporting Information). The thickness of the polymersome membrane is around 9.2 nm.<sup>[42]</sup> The polymersomes preserved their structural integrity after constant irradiation with red LED light compared with the non-irradiated polymersomes as observed by TEM micrographs (Figure 1). The integrity of the polymersomes under constant irradiation is further confirmed by DLS measurements taken

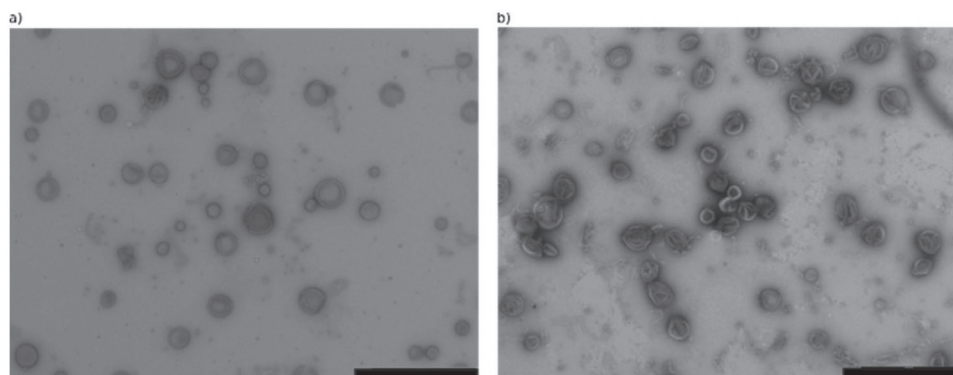


**Figure 1.** TEM micrographs of TPyCP containing polymersomes a) in Tris buffer before irradiation b) in Tris buffer after 2 h of constant irradiation with LED red light. Scale bars are 200 nm.

after 2 h of irradiation. Moreover the polymersomes preserve their architecture in cell media used for the cell viability and ESR studies (Figure S2, Supporting Information). The loading efficiency of our porphyrin into polymersomes, the removal of the TPyCP excess has monitored by fluorescence spectroscopy optimized and reported in our previous study. The unspecific uptake of the PS containing polymersomes and PS by mammalian cells is known and has been studied and optimized.<sup>[43]</sup> We know that the uptake takes place after 24 h incubation of the polymersomes with the cells and the final concentration range of the polymer is 0.25–0.1 mg mL<sup>-1</sup>. For this study we used the same experimental and concentration conditions to ensure the internalization of the compartments into the cells.<sup>[43–45]</sup>

## 2.2. ROS Generation in Solution

In the presence of triplet oxygen and upon irradiation, the main ROS which our porphyrin generates is <sup>1</sup>O<sub>2</sub>.<sup>[37]</sup> At the same time, TPyCP can also generate a very small amount of superoxide radical. Because of the small contribution of superoxide radical, when we discuss about ROS formed by TPyCP we refer to <sup>1</sup>O<sub>2</sub>. In order to investigate the <sup>1</sup>O<sub>2</sub> generation from the irradiated TPyCP free dissolved in tris buffer or encapsulated in polymersomes we used ESR with DMPO as spin trap.<sup>[46]</sup> The intensity of the ESR signal resulting from the spin trapping of hydroxyl radicals with DMPO was used to compare the level of ROS diffused through the polymersome membrane with that generated by TPyCP free in solution. Based on the mechanism already described in literature,<sup>[47]</sup> <sup>1</sup>O<sub>2</sub> generated by TPyCP is able to interact with DMPO as well as generate OH radicals from the aqueous media. The OH radicals are then able to form the

typical DMPO/OH adduct. Both reactions lead to the quartet signal. On that point we are not evaluating the contribution of these parallel reactions, since both are based on the <sup>1</sup>O<sub>2</sub> generation by TPyCP upon irradiation. First, we tested the free TPyCP (100 μM) after 0, 15, 30, 45, and 60 min of irradiation in the conditions described in the previous section. The spin trap we used is “ESR silent” when no specific free radicals are present, while in their presence it forms ESR active adducts. The ESR spectra with a pattern of four peaks (*g* = 2.005) with an intensity of 1:2:2:1 have been simulated (Figure 2a) by considering oxygen (O) as a central atom, one nitrogen (N) (a hyperfine coupling constant *a*<sub>N</sub> = 14.9 G) and one proton (a hyperfine coupling constant of *a*<sub>H</sub> = 14.9 G), typical of DMPO/OH adducts. The additional small contribution (<5%) detected, belongs to a combination of characteristic carbon-centered radical DMPO adduct and the oxidation of DMPO to DMPOX species since we know that TPyCP is able to produce a small fraction of superoxide radical. The contribution of this signal does not overlap with the quartet signal of DMPO/OH adduct which is of interest in this study. The possible formation of a DMPO superoxide adduct has not been detected because of its very short lifetime (<1 min). As expected, in the case of encapsulated porphyrin, the same DMPO/OH adducts were formed, but their associated ESR intensity was different over time. While the free TPyCP was able to rapidly generate ROS (Figure 2b), as indicated by the increase of the ESR signal after 15 min of irradiation, when encapsulated at the same concentration (100 μM) into PMOXA-PMDS-PMOXA polymersomes, a lower intensity ESR spectrum has been obtained (Figure 2c). ROS generated inside the cavity of the polymersomes need time to diffuse out, interact with DMPO, and form the radical adducts. As expected after 15 min of irradiation time, the polymer membrane acts as a diffusion

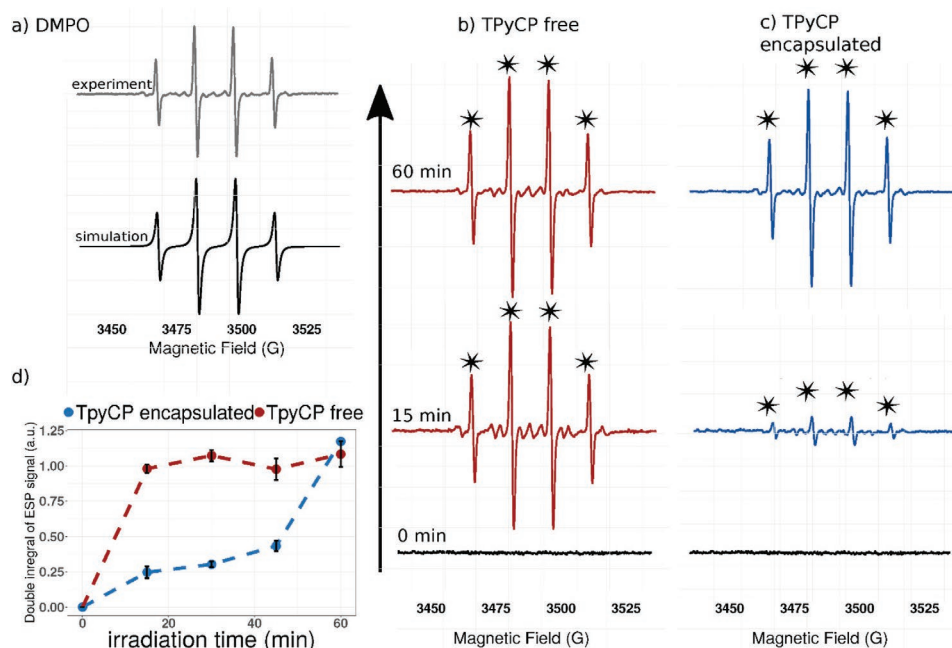


**Figure 2.** a) Experimental and simulated ESR spectra of DMPO/OH adducts formed in the presence of irradiated TPyCP (100 μM) b) ESR spectra of free and c) encapsulated TPyCP (100 μM) in polymersomes in three different time points of irradiation time 0, 15, and 60 min c,d) the double integral of ESR spectra of DMPO/OH adducts plotted against the irradiation time (min).

barrier for the ROS generated which causes a delay affecting the intensity of the ESR signal in the environment of the polymersomes. After approximately 45 min of irradiation time, the amount of generated ROS is high enough and therefore the effect of the polymer membrane is not affecting the intensity of the signal. Both free TPyCP and encapsulated generate continuously ROS as long as it is irradiated, as observed by the ESR spectra recorded after 60 min of irradiation (Figure 2d). In addition, the intensity of EPR spectra becomes almost equal for the free porphyrin and when encapsulated, after 60 min of irradiation (Figure 2d). Neither empty polymersomes nor tris buffer gave an ESR signal (Figure S5, Supporting Information). Also in the absence of irradiation (dark conditions) no ESR signal associated to the DMPO/OH adduct was obtained.

### 2.3. ROS Generation In Vitro

To further investigate the behavior of both free and encapsulated TPyCP, the intracellular ROS levels were determined by ESR with acyl-protected hydroxylamine, 1-acetoxy-3-carba-

moyl-2,2,5,5-tetramethylpyrrolidine, (ACP), commonly used for the detection of intracellular levels of ROS.<sup>[48]</sup> HeLa, HEK293T and HepG2 cells after internalization of the free and encapsulated TPyCP in various concentrations, respectively, were rinsed thoroughly with PBS to remove any extracellular TPyCP and then treated with ACP in its acyl-protected form. Once inside cells, ACP is deprotected by esterases and oxidized in the presence of cellular ROS to a stable nitroxide radical ESR active, which can be directly measured inside cells. The ESR spectra with a pattern of three peaks ( $g = 2.035$ ) with an intensity of 1:1:1 have been simulated by considering oxygen (O) as a central atom and one nitrogen (N) (a hyperfine coupling constants  $a_N = 16.1$  G) (Figure S12, Supporting Information). We used the double integral of the recorded ESR spectra to compare the signals intensity associated with a specific ROS level (Table S1, Supporting Information). All cell types (HeLa, HEK 293T, and HepG2) incubated without TPyCP species (control cells) or with empty polymersomes had very low intensity ESR spectra (Figure 3), characteristic of the nitroxide radical caused by the natural base-level of ROS in cells<sup>[46,48]</sup> It is important that a low irradiation dose has been used:  $1.32\text{--}5.28$  J  $\text{cm}^{-2}$  with that

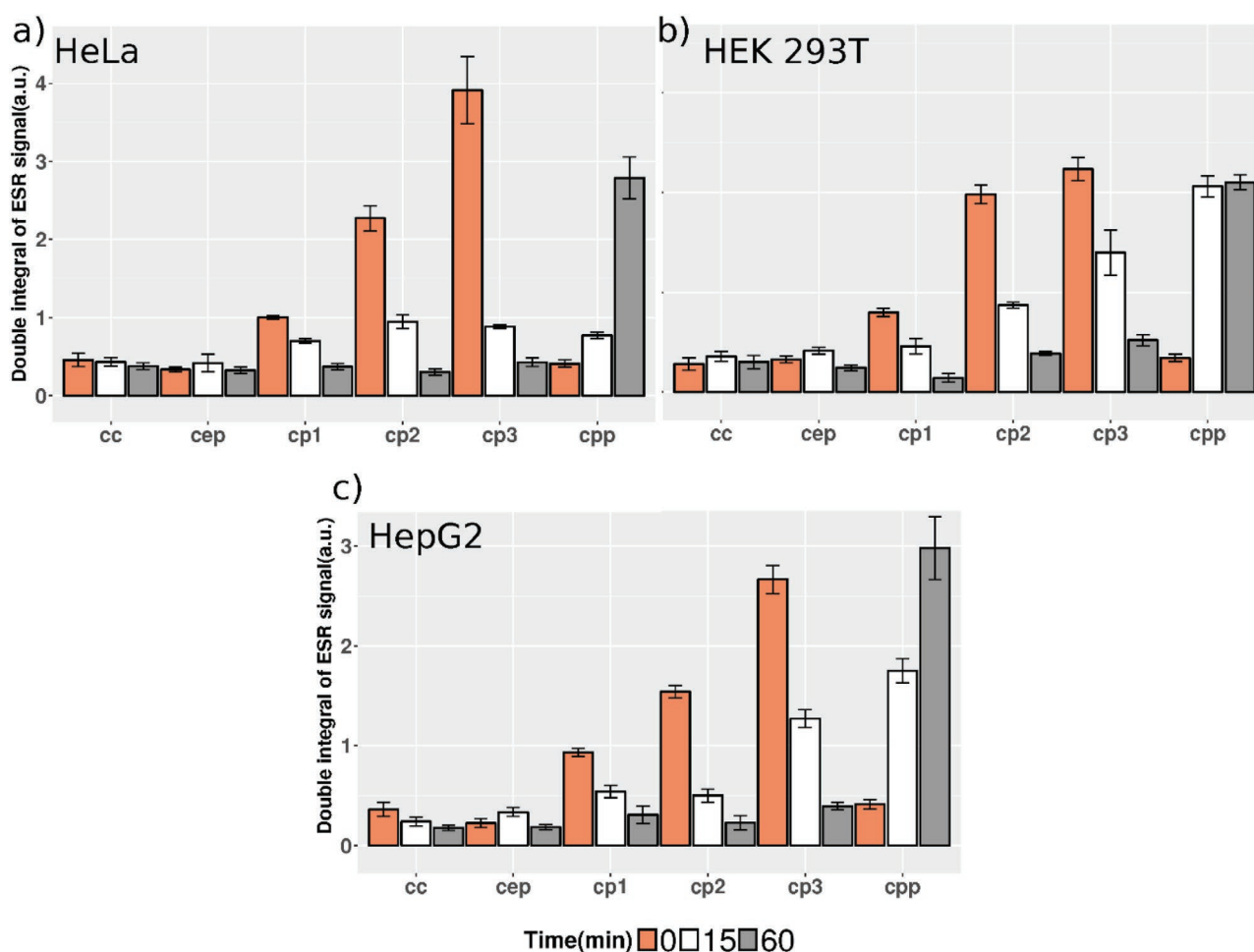


**Figure 3.** Double integral of the ESR intensity associated with the nitroxide ACP spin trap as obtained by the incubation of: a) HeLa b) HEK293 and c) HepG2 cells. The cell population is grouped by type: control cells (cc), cells incubated with empty polymersomes (cep), cells incubated with: 25 μM TPyCP (cp1), 50 μM TPyCP μM (cp2), 100 μM TPyCP (cp3), and cells incubated with 100 μM TPyCP-loaded polymersomes (cpp) for different irradiation times: 0 min (orange bars), 15 min (white bars), and 60 min (grey bars).



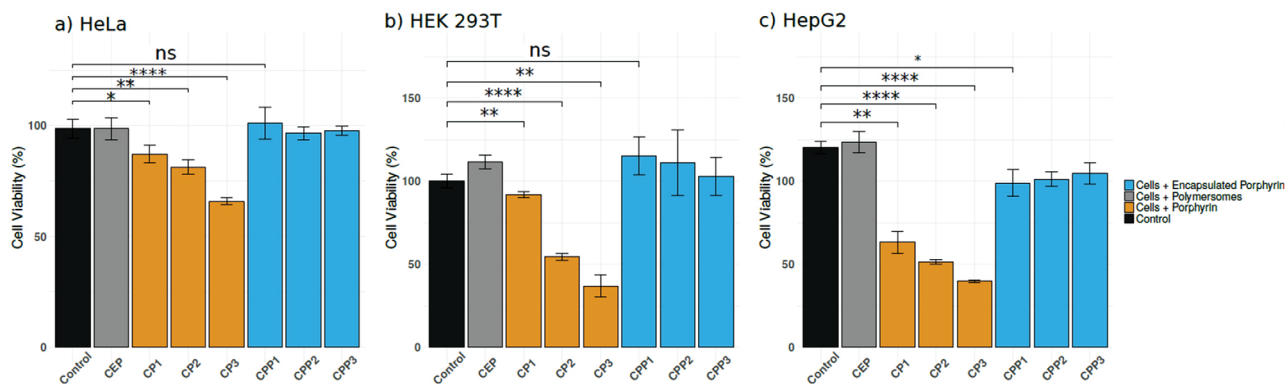


**Figure 4.** Cell viability in dark conditions of: a) HeLa b) HEK 293T and c) HepG2 cells. The cell population is grouped by type: control cells (cc, black bar), cells incubated with empty polymersomes (cep, grey bars) 25  $\mu\text{M}$  TPyCP (cp1) 50  $\mu\text{M}$  TPyCP (cp2) 100  $\mu\text{M}$  TPyCP (cp3) (orange bars) and cells incubated with TPyCP encapsulated into polymersomes 25  $\mu\text{M}$  TPyCP (cpp1) 50  $\mu\text{M}$  TPyCP (cpp2) 100  $\mu\text{M}$  TPyCP (cpp3) (blue bars).

being crucial for the in vitro evaluation of our system. For the cells incubated with increasing amounts of the free porphyrin (ranging from 25 up to 100  $\mu\text{M}$ ), the level of ROS was TPyCP-concentration dependent before irradiation (“dark conditions,”  $t = 0$  min). Elevated intracellular ROS levels are known to induce apoptosis via oxidative stress.<sup>[11]</sup> HeLa cells (Figure 3a) when incubated with free TPyCP in the three selected concentrations 25, 50, and 100  $\mu\text{M}$  show in comparison with the HEK 293T and HepG2 cells the highest ROS level at before irradiation. Moreover, the same cell line shows among all three the lowest level of ROS when TPyCP 100  $\mu\text{M}$  is encapsulated in polymersomes after 60 min of irradiation. HEK 293T cells (Figure 3b) on the other hand appear to have the highest level of ROS, when TPyCP 100  $\mu\text{M}$  is encapsulated in polymersomes, after 15 min of irradiation compared to HeLa and HepG2. At the same time, the level of detected ROS from HepG2 when incubated with TPyCP containing polymersomes increases stepwise from 0 to 15 min and from 15 to 60 min of irradiation time (Figure 3c). Despite these small differences, all three tested cell lines have shown fairly similar response. To avoid repetitions, we summarize the most important observations which apply for HeLa, HEK 293T, and HepG2 cells from ESR characterization of TPyCP free and encapsulated. In particular, an almost proportional relationship between the concentration of the free porphyrin and the amount of ROS generated in dark conditions was obtained compared with the control cells or cells incubated with empty polymersomes, characterized by a constant, very low intensity ESR signal. After 15 min of red light irradiation, the level of intracellular  $^1\text{O}_2$  generated by the free porphyrin decreased for all three concentrations used and the decrease continued after 60 min of irradiation (Figure 3). A possible explanation for this observation is the fact that even though our photosensitizer is stable under constant illumination in solution and generates  $^1\text{O}_2$  up to 48 h, when internalized in the cell environment, its effect might be hindered by the cell defense mechanisms. For instance, cells possess proteins able to dismantle aromatic compounds as porphyrins by electron transfer.<sup>[49–52]</sup> Additionally, if not the photosensitizer, the radical adducts formed in high amounts can also interfere with endogenous cell defense reactions.<sup>[53–56]</sup> As we observe this decrease in the ESR signal only when cells are incubated with

the free porphyrin, it indicates that the internalization of the free porphyrin into the cells and the consequent formation of the ESR adducts is outcompeted by the internal mechanisms of the cells. On the other hand, when cells were incubated with 100  $\mu\text{M}$  TPyCP-loaded polymersomes, the ROS level was similar to that of control cells at  $t = 0$  min, indicating that the encapsulation of porphyrins protects the cells from their intrinsic cytotoxicity. After 15 min of red light irradiation a significant increase of  $^1\text{O}_2$  levels has been obtained for the TPyCP-loaded polymersomes, which reached a maximum at irradiation time 60 min. This is a key observation: TPyCP encapsulated into polymersomes is able to generate ROS in continuously over time, that is, the higher the irradiation dose the higher the ROS production. On the other side, when the porphyrin is free in solution, the level of generated ROS is significantly decreasing. Therefore, encapsulation of the porphyrin into polymersomes not only protects the cells from its dark cytotoxicity but also facilitates in vitro the oxidative stress inducing apoptosis.

#### 2.4. Cell Viability in Dark Conditions

In order to evaluate the intrinsic cytotoxicity of TPyCP both free and encapsulated in PMOXA<sub>6</sub>-PDMS<sub>34</sub>-PMOXA<sub>6</sub> polymersomes, we used the MTS assay in three cell lines (HEK293T, HeLa, and HepG2). We first tested the so called “dark cytotoxicity,” which represents the impact of the free and encapsulated porphyrin, respectively, on cell viability under dark conditions. The cells were incubated in the presence of increasing concentrations of TPyCP (free and encapsulated, ranging from 25 to 100  $\mu\text{M}$ ) dissolved in a 50:50 mixture of tris buffer and cell media. To address the possible interference of the polymersome membrane with the cells, we also added empty polymersomes rehydrated in tris buffer. After 24 h incubation, the viability of HEK293T, HeLa, and HepG2 cells without and with TPyCP (free or encapsulated inside polymersomes) was evaluated (Figure 4). Free TPyCP (all used concentrations) reduced significantly the viability of HeLa, HEK 293T, and HepG2 cells. More specifically, the cell viability of HeLa cells was reduced up to 26% for the highest concentration of free porphyrin (100  $\mu\text{M}$  TPyCP) (Figure 4a) and in

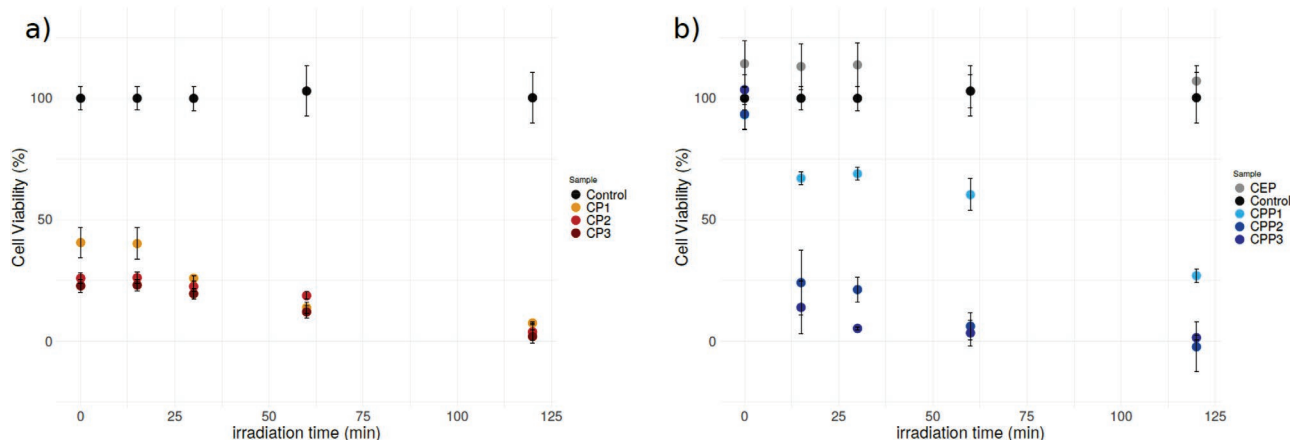


**Figure 5.** HeLa cell viability plotted as a function of irradiation time (min): control cells (cc, black points), cells incubated with empty polymersomes (cep, grey points), cells incubated with: 25  $\mu\text{M}$  TPYCP (cp, yellow points), 50  $\mu\text{M}$  TPYCP (cp2, red points), 100  $\mu\text{M}$  TPYCP (cp3, dark red points) and cells incubated with: 25  $\mu\text{M}$  TPYCP (cpp, light blue points), 50  $\mu\text{M}$  TPYCP (cpp2, blue points), 100  $\mu\text{M}$  TPYCP (cpp3, dark blue)-loaded polymersomes a) the subset of the cell population incubated with free porphyrin and b) the subset of the population incubated with the encapsulated porphyrin.

comparison to HEK 293T and HepG2 the dark toxicity of the porphyrin seems to be stronger. The decrease of cell viability of HEK 293 T (Figure 4b) was even higher, reaching 56% for 100  $\mu\text{M}$  free TPYCP. In the case of HepG2 cells (Figure 4c), the cytotoxicity of free TPYCP was significantly higher: even at the lowest concentration used (25  $\mu\text{M}$ ), the viability was reduced by 49% and for the highest porphyrin concentration (100  $\mu\text{M}$ ), the reduction of cell viability reached 71%. As already observed in the previous section from the ESR in vitro data (Figure 3), the cell viability assay shows that all the three cell lines used for our study have analogous results when incubated with free encapsulated TPYCP in dark conditions. While the cytotoxic effect of the free TPYCP was observed for all cell lines, with different degrees of toxicity, when TPYCP was encapsulated inside polymersomes (with similar concentration as the free porphyrin) there was no significant change in cell viability. Note that we observed only for HepG2 cells a slight decrease in viability upon incubation for 24 h with TPYCP containing polymersomes (7.1–9.8%) (Figure 4c), but this was significantly lower than the one related to the free porphyrin (where almost 71% of cells were apoptotic).

The viability assays indicate that polymersomes efficiently shield the porphyrin and reduce its intrinsic dark cytotoxicity, whilst allowing ROS generated in situ to diffuse through the synthetic membrane in a controlled manner. In addition, a great advantage of our system is that the irradiation dose ranges from 1.3 up to 5.8  $\text{J cm}^{-2}$  (Table S2, Supporting Information), which is significantly low in comparison to the dose conditions related to a laser light source<sup>[40,57]</sup> and within the normal range used with LED irradiation.<sup>[24,57,58]</sup>

## 2.5. Cell Viability upon Irradiation

To evaluate the bio-functionality of the TPYCP-loaded polymersomes as an efficient ROS source in mammalian cells, we determined the cells viability as a function of the irradiation time. The cells were co-cultured with free- and polymersome-encapsulated TPYCP at the same concentrations as above and

exposed to LED irradiation (red light  $\lambda = 660 \text{ nm}$ ). The cell viability was determined by MTS assay and then plotted against irradiation time. HeLa cells viability upon incubation with increasing concentrations of free TPYCP without irradiation significantly reduced the cell viability ( $t = 0 \text{ min}$ , Figure 5).

Upon irradiation the population of alive HeLa cells reduces up to 99%. On the contrary, HeLa cells incubated with TPYCP encapsulated into  $\text{PMOXA}_6\text{-PDMS}_{34}\text{-PMOXA}_6$  polymersomes (in concentrations ranging from 25 up to 100  $\mu\text{M}$ ) without irradiation showed no cytotoxicity (Figure 4a) similar to the cells which did not contain any TPYCP. After 15 min of irradiation, the singlet oxygen produced in the cavity of polymersomes diffuses out and induces a reduction of the cell viability of 69% (45 min irradiation) rising to 98%. The advantage of encapsulating TPYCP inside polymersomes is that the released singlet oxygen and apoptosis takes place in a controlled manner: only upon irradiation can the porphyrin-loaded polymersomes produce ROS, while without irradiation the system has no cytotoxicity. Control experiments with HeLa cells incubated with empty polymersomes or cultured in the absence of any TPYCP (free or encapsulated) indicated that the cell viability was not affected after 2 h of irradiation ( $\lambda = 660 \text{ nm}$ ).

Similar behavior was observed for HEK 293T and HepG2 (Figures S13 and S14, Supporting Information) cells. More specifically, for HEK 293T cells co-cultured with free TPYCP the cell viability was reduced to 52% before exposure to red LED light and to 3% after 15 min of irradiation (Figure S13, Supporting Information). In the case of TPYCP-loaded polymersomes, which were no cytotoxic without irradiation, as the irradiation time increases, the viability drops after 15 min to 59% and continues reducing to 1.5% after 60 min irradiation (Figure S13c, Supporting Information). HepG2 cells show a response close to HEK293T (Figure S14, Supporting Information): without irradiation, the free porphyrin is very cytotoxic (Figure S14b, Supporting Information) while the encapsulated one has no cytotoxicity (Figure S14c, Supporting Information), the cell viability reaching 93% in comparison to the control cells (untreated with porphyrin). After irradiation, the population of living cells incubated with TPYCP-loaded polymersomes

reduces by 56% (15 min irradiation) and ends up at 1–2% after 60 min of irradiation. These viability assays indicate that our porphyrin loaded polymersomes reduce in vitro the cell viability in higher efficacy compared to similar results obtained by other studies with similar systems of porphyrin containing polymersome.<sup>[22,23]</sup> These results are in very good agreement with the behavior of the free and encapsulated porphyrin obtained by spin trap ESR. Combining an assay for cell viability with a very sensitive technique for <sup>1</sup>O<sub>2</sub> detection, such as ESR, gave us the opportunity to successfully correlate the photoactivation caused by irradiated TPyCP and the cell death by oxidative stress. While in our previous study we reported the photoactivation of dioxygen by TPyCP against E. coli bacteria, which do not have a complex defense mechanisms against drugs or aromatic compounds, by now we successfully induced apoptosis of mammalian cells in a controlled fashion and under low dosage of irradiation.

### 3. Conclusions

We have demonstrated that the encapsulation of TPyCP porphyrin into polymersomes based on amphiphilic triblock copolymers is crucial to decrease the intrinsic toxicity of porphyrins, and influence the photodynamic therapy efficacy. Once up taken by cells, the encapsulated porphyrin was able to produce ROS “on demand” upon irradiation with red LED light. After diffusion through the synthetic membrane in the polymersomes environment, ROS induced a significant reduction of the viability of HeLa, HEK 293T, and HepG2 cells. TPyCP porphyrin-loaded polymersomes showed no or very low dark cytotoxicity, while the free porphyrin had a significant dark cytotoxicity leading to cell death in an uncontrolled way. The results obtained by ESR and MTS cell viability assay are in good agreement, strongly indicating that our system is non-toxic and facilitates the long-term ROS generation in vitro. We can further improve our system in order to make it more specific and applicable not only in vitro but also in vivo.

### 4. Experimental Section

**Polymersome Formation:** Polymersome formation in presence of TPyCP and purification has been previously reported.<sup>[34]</sup> For the formation of the polymersomes, the amphiphilic triblock copolymer PMOXA<sub>6</sub>-PDMS<sub>34</sub>-PMOXA<sub>6</sub> was used and prepared as previously described.<sup>[41]</sup> The film rehydration method was followed. Polymer (5 mg) was dissolved in EtOH (1 mL) and dried under vacuum to form a polymer film on the inner bottom of a 5 mL round glass flask. The polymer film was rehydrated with tris (hydroxymethyl) aminomethane (Tris) buffer (50 mM, pH 7.6) at room temperature for 48 h in the dark in the presence or absence of a 25, 50, or 100 μM TPyCP solution, respectively. The suspension was then sequentially extruded through 0.2 and 0.1 μm Nucleopore Track-Etch membranes from Whatman using an Avanti Extruder (Avanti Polar Lipids, USA). Any TPyCP left in solution was separated from the polymersomes containing TPyCP by passage through a HiTrap desalting column (Sephadex G-25 Superfine, GE Healthcare, UK) or a 20 cm<sup>3</sup> in-house prepacked column (Sephacrose 2B, Sigma-Aldrich).

**Dynamic Light Scattering:** The polymersomes obtained were characterized by dynamic light scattering measurements (DLS) and measured in a Zetaziser Nano (Malvern) at 25 °C equipped with a

HeNe laser ( $\lambda = 633$  nm). The samples were diluted ten times and left to equilibrate for 120 s. The same samples were then recovered and subjected to transmission electron microscopy (TEM).

**Transmission Electron Microscopy:** For visualization, 10 μL of a polymersome solution was negatively stained with 2% aqueous uranyl acetate solution, deposited on a carbon-coated copper grid, and then examined with a transmission electron microscope (Philips Morgani 268 D) operating at 80 kV.

**Cell Culturing:** HeLa, Hek 293T, and HepG2 were cultured for both MTS viability assay and ESR measurements. The cells were cultured in Dulbecco's Modified Eagle Medium with GlutaMAX-1 and supplemented with 10% Fetal calf serum (FCS) and 1% penicillin/Streptomycin (100 units mL<sup>-1</sup> penicillin and 100 μg mL<sup>-1</sup> Streptomycin). Cells were kept the incubator with temperature and humidity control: 5% CO<sub>2</sub> at 37 °C.

**MTS Cell Viability Assay:** HeLa, Hek 293T, and HepG2 cells were cultured at a density of  $5 \times 10^3$  cells per well in a clear 96-well plate for 24 h. Cells then were incubated for another 24 h in the presence of 25, 50, and 100 μM TPyCP dissolved in cell media (Cp1, Cp2, Cp3 are the respective short names of each case) 100 μM TPyCP-loaded polymersomes (Cpp) and empty polymersomes (Cep). Afterward, the medium was removed and the cells were washed with PBS and fresh medium was given to the cells. The cells were irradiated under the LED lamp set at 660 nm wavelength from the top at a fixed distance so all wells are irradiated equally for 0, 15, 30, and 60 min. Afterward, the MTS assay (<https://www.promega.com/-/media/files/resources/protocols/technical-bulletins/0/celltiter-96-aqueous-one-solution-cell-proliferation-assay-system-protocol.pdf>) was performed to determine the cell viability. After 2 h of MTS reagent incubation, absorbance was measured at 490 nm, as indicated in the Promega protocol, using a Spectramax plate reader (Molecular Devices LLC, USA). Background absorbance, measured in control wells containing all assay components except cells, and was subtracted from each well. Control cells (CC) which were incubated with nothing but cell media were set as 100% viability and all the other recorded values were normalized according to this. For the data analysis and the statistical *t*-test we used Rstudio using the two-tailed Student's *t*-test and the ( $p \leq 0.001$  is significant with three stars,  $p \leq 0.01$  is significant with two stars,  $p \leq 0.05$  is significant with one star and  $p > 0.05$  is not significant (ns),  $n = 4$ ). We use control cells as a reference population and compare each other population with it.

**ESR for the TPyCP Free in Solution and Encapsulated:** DMPO spin trap was purchased from Sigma-Aldrich in highest purity and was used for the ESR measurements. More specifically, 0.5 mL of TPyCP 100 μM dissolved in Tris-buffer, polymersomes containing 100 μM TPyCP, empty polymersome solution in Tris buffer as well as Tris buffer alone was mixed with 10 μL of DMPO solution 1 M also dissolved in Tris-buffer. Each sample was irradiated for 0, 15, 60, and 120 min with the LED lamp and then ESR spectra were recorded. ESR measurements were performed on a Bruker CW ESR Eleksys-500 spectrometer equipped with a variable temperature unit. The spectra were recorded at 298 K with the following parameters: scans 10, sweep width 100.0 G, center field 3480.00 G, the microwave power 0.002 Watt, and frequency of 9.77 GHz. The modulation amplitude was 1.0 G. ESR simulations were performed with XSophe (v 1.1.4.1, Bruker).

**ESR of Cells Incubated with TPyCP free in Solution and Encapsulated Inside Polymersomes:** ACP spin trap was purchased from Noxygen in highest purity and then used for in vitro detection of intracellular ROS. HeLa, HEK 293T, and HepG2 cells were cultured the same way as described for the MTS viability assay. After 24 h incubation with 25, 50, and 100 μM TPyCP dissolved in cell media (Cp1, Cp2, Cp3 are the respective short names of each case) 100 μM TPyCP loaded polymersomes (Cpp) and empty polymersomes (Cep), cells were washed twice with Phosphate buffer saline (PBS) (from Gibco pH 7.4) re-suspended in fresh cell media and then incubated for 90 min with 10 mM ACP. Afterward, cells have been washed PBS, trypsinized, centrifuged for 5 min in 500 rpm, and re-suspended in 1 mL fresh media. Then they were irradiated under the LED lamp for 0, 15, and 60 min and 0.5 mL was transferred into a Suprasil tube for ESR measurement. The



ESR spectra were recorded at 298 K with the following parameters: scans 6, sweep width 100.0 G, center field 3480.00 G, the microwave power 0.002 Watt and frequency of 9.87 GHz. The modulation amplitude was 1.0 G. ESR simulations were performed with XSophe (v 1.1.4.1, Bruker).

**LED Irradiation Conditions:** The LED light source used to initiate the ROS production from the TPycP was a THORLABS 4-Wavelength High-Power LED Source LED4D067 ([https://www.thorlabs.com/newgrouppage9.cfm?objectgroup\\_id=3836](https://www.thorlabs.com/newgrouppage9.cfm?objectgroup_id=3836)). Irradiation at 660 nm and 990 mW was set. The irradiation intensity was determined with a LED light intensity detector (LT45 Extch) in lux and then converted to  $\text{J cm}^{-2}$ .

## Supporting Information

Supporting Information is available from the Wiley Online Library or from the author.

## Acknowledgements

The authors acknowledge the Swiss National Science Foundation, the NCCR Molecular Systems Engineering, Swiss Nanoscience Institute (SNI) and the University of Basel for financial support. Dr. Samuel Lörcher is thanked for polymer synthesis and fruitful discussions, Gabriele Persy for TEM-measurements, Dr. Ioana Craciun for discussions and training regarding cell culturing and Dr. Cora-Ann Schoenberger for proofreading the manuscript.

## Conflict of Interest

The authors declare no conflict of interest.

## Keywords

nanocarrier, photoactivation, polymersomes, porphyrin, reactive oxygen species delivery

Received: August 8, 2019

Revised: October 3, 2019

Published online:

- [1] H. Ye, Y. Zhou, X. Liu, Y. Chen, S. Duan, R. Zhu, Y. Liu, L. Yin, *Biomacromolecules* **2019**, *20*, 2441.
- [2] K. Ding, Y. Zhang, W. Si, X. Zhong, Y. Cai, J. Zou, J. Shao, Z. Yang, X. Dong, *ACS Appl. Mater. Interfaces* **2018**, *10*, 238.
- [3] D. E. J. G. Dolmans, D. Fukumura, R. K. Jain, *Nat. Rev. Cancer* **2003**, *3*, 380.
- [4] F. Hammerer, F. Poyer, L. Fourmois, S. Chen, G. Garcia, M.-P. Teulade-Fichou, P. Maillard, F. Mahuteau-Betzer, *Bioorg. Med. Chem.* **2018**, *26*, 107.
- [5] B. Wu, X.-Q. Li, T. Huang, S.-T. Lu, B. Wan, R.-F. Liao, Y.-S. Li, A. Baidya, Q.-Y. Long, H.-B. Xu, *Biomater. Sci.* **2017**, *5*, 1746.
- [6] M. A. Rajora, J. W. H. Lou, G. Zheng, *Chem. Soc. Rev.* **2017**, *46*, 6433.
- [7] X. Xue, A. Lindstrom, Y. Li, *Bioconjugate Chem.* **2019**, *30*, 1585.
- [8] M. E. Alea-Reyes, M. Rodrigues, A. Serrà, M. Mora, M. L. Sagristá, A. González, S. Durán, M. Duch, J. A. Plaza, E. Vallés, D. A. Russell, L. Pérez-García, *RSC Adv.* **2017**, *7*, 16963.
- [9] K. Nawalany, A. Rusin, M. Kępczyński, A. Mikhailov, G. Kramer-Marek, M. Śnietura, J. Połtowicz, Z. Krawczyk, M. Nowakowska, *J. Photochem. Photobiol., B* **2009**, *97*, 8.
- [10] C. Perotti, H. Fukuda, G. DiVenosa, A. J. MacRobert, A. Batlle, A. Casas, *Br. J. Cancer* **2004**, *90*, 1660.
- [11] J. Tian, W. Zhang, *Prog. Polym. Sci.* **2019**, *95*, 65.
- [12] H. Abrahamse, C. A. Kruger, S. Kadanyo, A. Mishra, *Photomed. Laser Surg.* **2017**, *35*, 581.
- [13] U. S. Chung, J.-H. Kim, B. Kim, E. Kim, W.-D. Jang, W.-G. Koh, *Chem. Commun.* **2016**, *52*, 1258.
- [14] G. Lan, K. Ni, W. Lin, *Coord. Chem. Rev.* **2019**, *379*, 65.
- [15] O. Penon, M. J. Marín, D. A. Russell, L. Pérez-García, *J. Colloid Interface Sci.* **2017**, *496*, 100.
- [16] O. Penon, T. Patiño, L. Barrios, C. Nogués, D. B. Amabilino, K. Wurst, L. Pérez-García, *ChemistryOpen* **2015**, *4*, 127.
- [17] B. I. Lee, S. Lee, Y. S. Suh, J. S. Lee, A. Kim, O.-Y. Kwon, K. Yu, C. B. Park, *Angew. Chem., Int. Ed.* **2015**, *54*, 11472.
- [18] S. Hameed, P. Bhattarai, X. Liang, N. Zhang, Y. Xu, M. Chen, Z. Dai, *Theranostics* **2018**, *8*, 5501.
- [19] J. Massiot, V. Rosilio, A. Makky, *J. Mater. Chem. B* **2019**, *7*, 1805.
- [20] G. Fuhrmann, A. Serio, M. Mazo, R. Nair, M. M. Stevens, *J. Controlled Release* **2015**, *205*, 35.
- [21] J. Massiot, V. Rosilio, N. Ibrahim, A. Yamamoto, V. Nicolas, O. Kononov, M. Tanaka, A. Makky, *Chem. Eur. J.* **2018**, *24*, 19179.
- [22] M. Spulber, P. Baumann, S. S. Saxer, U. Pielers, W. Meier, N. Bruns, *Biomacromolecules* **2014**, *15*, 1469.
- [23] L. Xu, L. Liu, F. Liu, H. Cai, W. Zhang, *Polym. Chem.* **2015**, *6*, 2945.
- [24] V. Ibrahimova, S. A. Denisov, K. Vanvarenberg, P. Verwilt, V. Préat, J.-M. Guigner, N. D. McClenaghan, S. Lecommandoux, C.-A. Fustin, *Nanoscale* **2017**, *9*, 11180.
- [25] C. G. Palivan, R. Goers, A. Najer, X. Zhang, A. Car, W. Meier, *Chem. Soc. Rev.* **2016**, *45*, 377.
- [26] P. Baumann, V. Balasubramanian, O. Onaca-Fischer, A. Sienkiewicz, C. G. Palivan, *Nanoscale* **2013**, *5*, 217.
- [27] *Modern Techniques for Nano- and Microreactors/-Reactions* (Ed: F. Caruso), Springer Berlin Heidelberg, Berlin, Heidelberg **2010**, p. 229.
- [28] P. P. Ghoroghchian, P. R. Frail, K. Susumu, D. Blessington, A. K. Brannan, F. S. Bates, B. Chance, D. A. Hammer, M. J. Therien, *Proc. Natl. Acad. Sci. U. S. A.* **2005**, *102*, 2922.
- [29] P. P. Ghoroghchian, J. J. Lin, A. K. Brannan, P. R. Frail, F. S. Bates, M. J. Therien, D. A. Hammer, *Soft Matter* **2006**, *2*, 973.
- [30] P. P. Ghoroghchian, P. R. Frail, K. Susumu, T.-H. Park, S. P. Wu, H. T. Uyeda, D. A. Hammer, M. J. Therien, *J. Am. Chem. Soc.* **2005**, *127*, 15388.
- [31] G. P. Robbins, M. Jimbo, J. Swift, M. J. Therien, D. A. Hammer, I. J. Dmochowski, *J. Am. Chem. Soc.* **2009**, *131*, 3872.
- [32] L. E. Sinks, G. P. Robbins, E. Roussakis, T. Troxler, D. A. Hammer, S. A. Vinogradov, *J. Phys. Chem. B* **2010**, *114*, 14373.
- [33] D. H. Levine, P. P. Ghoroghchian, J. Freudenberg, G. Zhang, M. J. Therien, M. I. Greene, D. A. Hammer, R. Murali, *Methods* **2008**, *46*, 25.
- [34] A. Lanzilotto, M. Kyropoulou, E. C. Constable, C. E. Housecroft, W. P. Meier, C. G. Palivan, *J. Biol. Inorg. Chem.* **2018**, *23*, 109.
- [35] P. Baumann, M. Spulber, I. A. Dinu, C. G. Palivan, *J. Phys. Chem. B* **2014**, *118*, 9361.
- [36] F. Axthelm, O. Casse, W. H. Koppenol, T. Nauser, W. Meier, C. G. Palivan, *J. Phys. Chem. B* **2008**, *112*, 8211.
- [37] V. Chimisso, V. Maffei, D. Hürlimann, C. G. Palivan, W. Meier, *Macromol. Biosci.* **2019**, *1900257*, 2019.
- [38] Konishcheva, E. , Daubian, D. , Gaitzsch, J. , Meier, W. *Helv. Chim. Acta* **2018**, *101*, e1700287.
- [39] T. S. Mang, *Photodiagn. Photodyn. Ther.* **2004**, *1*, 43.
- [40] S. I. Dikalov, D. G. Harrison, *Antioxid. Redox Signaling* **2014**, *20*, 372.
- [41] S. Lörcher, W. Meier, *Eur. Polym. J.* **2017**, *88*, 575.
- [42] F. Itel, A. Najer, C. G. Palivan, W. Meier, *Nano Lett.* **2015**, *15*, 3871.



- [43] T. Einfalt, D. Witzigmann, C. Edlinger, S. Sieber, R. Goers, A. Najer, M. Spulber, O. Onaca-Fischer, J. Huwyler, C. G. Palivan, *Nat. Commun.* **2018**, 9, 1127.
- [44] P. U. Richard, I. Craciun, J. Gaitzsch, L. Weiner, C. G. Palivan, *Helv. Chim. Acta* **2018**, 101, e1800064.
- [45] A. Belluati, I. Craciun, J. Liu, C. G. Palivan, *Biomacromolecules* **2018**, 19, 4023.
- [46] M. Roesslein, C. Hirsch, J.-P. Kaiser, H. Krug, P. Wick, *Int. J. Mol. Sci.* **2013**, 14, 24320.
- [47] P. Bilski, K. Reszka, M. Bilaska, C. F. Chignell, *J. Am. Chem. Soc.* **1996**, 118, 1330.
- [48] A. Ueda, A. Hirayama, S. Nagase, M. Inoue, T. Oteki, M. Aoyama, H. Yokoyama, *Free Radical Res.* **2007**, 41, 823.
- [49] B. Levine, Eating Oneself, Uninvited Guests, *Cell* **2005**, 120, 159.
- [50] C.-H. Lecellier, *Science* **2005**, 308, 557.
- [51] P. V. Maillard, C. Ciaudo, A. Marchais, Y. Li, F. Jay, S. W. Ding, O. Voinnet, *Science* **2013**, 342, 235.
- [52] S. Xia, X. Zhang, S. Zheng, R. Khanabdali, B. Kalionis, J. Wu, W. Wan, X. Tai, *J. Immunol. Res.* **2016**, 2016, 1.
- [53] N. Babić, F. Peyrot, *Magnetochemistry* **2019**, 5, 13.
- [54] N. Bézière, Y. Frapart, A. Rockenbauer, J.-L. Boucher, D. Mansuy, F. Peyrot, *Free Radicals Biol. Med.* **2010**, 49, 437.
- [55] H. Hong, J. Sun, W. Cai, *Free Radicals Biol. Med.* **2009**, 47, 684.
- [56] M. Pignitter, A. Gorren, S. Nedeianu, K. Schmidt, B. Mayer, *Free Radicals Biol. Med.* **2006**, 41, 455.
- [57] J.-H. Li, Z.-Q. Chen, Z. Huang, Q. Zhan, F.-B. Ren, J.-Y. Liu, W. Yue, Z. Wang, *Oncol. Lett.* **2013**, 5, 702.
- [58] J. Carneiro, A. Gonçalves, Z. Zhou, K. E. Griffin, N. E. M. Kaufman, M. da G. H. Vicente, *Lasers Surg. Med.* **2018**, 50, 566.